

Article

Valorization of Rice Straw into Cellulose Microfibers for the Reinforcement of Thermoplastic Corn Starch Films

Pedro A. V. Freitas ^{1,*}, Carla I. La Fuente Arias ^{1,2} , Sergio Torres-Giner ¹ , Chelo González-Martínez ¹ 
and Amparo Chiralt ¹ 

¹ Research Institute of Food Engineering for Development (IIAD), Universitat Politècnica de València (UPV), 46022 Valencia, Spain; carlalfa@usp.br (C.I.L.F.A.); storresginer@upv.es (S.T.-G.); cgonza@tal.upv.es (C.G.-M.); dchiralt@tal.upv.es (A.C.)

² Department of Agri-Food Industry, Food and Nutrition (LAN), School of Agriculture Luiz de Queiroz (ESALQ), Universidade de Sao Paulo, Piracicaba 13418-900, Brazil

* Correspondence: pedvidef@doctor.upv.es

Abstract: In the present study, agro-food waste derived rice straw (RS) was valorized into cellulose microfibers (CMFs) using a green process of combined ultrasound and heating treatments and were thereafter used to improve the physical properties of thermoplastic starch films (TPS). Mechanical defibrillation of the fibers gave rise to CMFs with cumulative frequencies of length and diameters below 200 and 5–15 μm , respectively. The resultant CMFs were successfully incorporated at 1, 3, and 5 wt% into TPS by melt mixing and also starch was subjected to dry heating (DH) modification to yield TPS modified by dry heating (TPSDH). The resultant materials were finally shaped into films by thermo-compression and characterized. It was observed that both DH modification and fiber incorporation at 3 and 5 wt% loadings interfered with the starch gelatinization, leading to non-gelatinized starch granules in the biopolymer matrix. Thermo-compressed films prepared with both types of starches and reinforced with 3 wt% CMFs were more rigid (percentage increases of ~215% for TPS and ~207% for the TPSDH), more resistant to break (~100% for TPS and ~60% for TPSDH), but also less extensible (~53% for TPS and ~78% for TPSDH). The incorporation of CMFs into the TPS matrix at the highest contents also promoted a decrease in water vapor (~15%) and oxygen permeabilities (~30%). Finally, all the TPS composite films showed low changes in terms of optical properties and equilibrium moisture, being less soluble in water than the TPSDH films.

Keywords: waste valorization; rice straw; thermoplastic starch; cellulose; thermal modification; microcomposites



Citation: Freitas, P.A.V.; Arias, C.I.L.F.; Torres-Giner, S.; González-Martínez, C.; Chiralt, A. Valorization of Rice Straw into Cellulose Microfibers for the Reinforcement of Thermoplastic Corn Starch Films. *Appl. Sci.* **2021**, *11*, 8433. <https://doi.org/10.3390/app11188433>

Academic Editor: Giorgia Spigno

Received: 31 July 2021

Accepted: 9 September 2021

Published: 11 September 2021

Publisher's Note: MDPI stays neutral with regard to jurisdictional claims in published maps and institutional affiliations.



Copyright: © 2021 by the authors. Licensee MDPI, Basel, Switzerland. This article is an open access article distributed under the terms and conditions of the Creative Commons Attribution (CC BY) license (<https://creativecommons.org/licenses/by/4.0/>).

1. Introduction

Today, the proper management of agro-industrial wastes is an essential socioeconomic and environmental issue. Most of these residues or by-products, generated in large quantities globally, are currently discarded or burned in the harvest fields [1]. In this sense, the use and valorization of agro-industrial waste into added-value materials are an emerging challenge that seeks to minimize environmental problems and promote the correct residue disposal. Agro-food and industrial waste derived biomass is essentially composed of lignocellulosic fractions, which are constituent biopolymers, such as cellulose, hemicellulose, and lignin [2,3]. Due to its renewability and biodegradability, the use of lignocellulosic-rich wastes can yield environmentally friendly materials through cost-effective processes with low environmental impact [4,5]. Several authors have reported the use of plant residues to obtain lignocellulosic fractions with potential application for biodiesel production [6], catalysts for biodiesel synthesis [7], antioxidant and antimicrobial materials [8,9] as well as reinforcing agents [10,11]. Particularly, cellulose and its derivatives extracted from biomass, such as cellulose microfibers (CMFs) and cellulose nanofibers, are highlighted renewable materials at the micro- and nanoscale, respectively, with low density, good compatibility,

and excellent mechanical properties [12]. Thus, these lignocellulosic fractions can be used as reinforcing fillers of biopolymers in green composites for food packaging applications.

After harvesting the rice grain (*Oryza sativa* L.), one of the most important primary crops, large quantities of rice straw (RS) are obtained worldwide. In fact, the annual rice production is estimated at 782 million tons and 1 kg of rice grain yields approximately 1.5 kg of RS [13,14]. Generally, RS is directly burned in the paddies, which intensifies air pollution and damages soil feasibility and population health. Therefore, constant efforts are currently being made to propose different management approaches for this biomass waste [14,15]. Since RS is a lignocellulosic material that is composed of approximately 39% cellulose, 20% lignin, 23% hemicellulose, and 15% ashes, this waste derived biomass can be used to obtain several renewable added-value materials with interesting properties [16]. Among the most practical alternatives, RS can be valorized into CMFs by different extraction methods. Typically, CMFs from RS has a strong crystalline structure and low density, which can be used as reinforcing agent in biodegradable polymers instead to petroleum derived plastics [2,17].

Starch is a semicrystalline biopolymer consisting of linear and branched chains of D-glucopyranose units known as amylose and amylopectin, respectively [18]. The proportion of both constituents varies according to the source, from which the most common are cassava, maize, sweet potato, rice, oats, and peas [19,20]. Starch is widely investigated for several applications due to its renewability, biodegradability, low cost, availability, and biocompatibility [21–23]. In its native state, starch can be processed with a plasticizer in an extruder at temperatures between 140 and 160 °C and high pressure, giving rise to an amorphous material with thermoplastic behavior [21]. Although thermoplastic starch (TPS) films are excellent barriers to lipids, oxygen, and carbon dioxide, their use in food packaging is still limited since the barrier and mechanical properties are highly dependent on moisture content [18,24,25]. To overcome these shortcomings, the preparation of biodegradable TPS films reinforced with CMFs obtained from agro-industrial wastes is an interesting alternative. Previous studies have reported that the incorporation of cellulosic materials in TPS-based green composite films exhibited enhanced mechanical properties [20,26], water vapor [27] and oxygen gas barrier [22], and thermal stability [28]. These recent advances indicate the significance and potential of green composites from starch and cellulose micro- and nanofibrils in the development of sustainable and cost-effective materials for food packaging [26,29] and other uses [30], from semistructural applications to biofoams or reinforcing adhesives. Likewise, another strategy to modify and/or improve the properties of TPS films is pre-treating the starch in its native state by the dry heating (DH) method. The so-called DH modification is a green physical pre-treatment that involves dry heating of native starch at temperatures between 110 and 150 °C for 1 to 4 h [31,32]. This method is very promising since it is simple, fast, does not produce effluents, and can modify the original physicochemical properties of native starch to produce materials with improved properties [32–34].

Thus, the objective of this work was to study the morphogeometric characteristics of CMFs obtained from waste derived RS, before and after fiber grinding, and its subsequent incorporation by melt mixing into TPS. Prior to melt mixing, native starch was also subjected to DH modification to yield thermoplastic dry heated corn starch (TPSDH). The resultant doughs of TPS and TPSDH filled with CMFs were thereafter shaped into films by thermo-compression and characterized in terms of their morphological characteristics, barrier properties, water solubility, water uptake, thermal behavior, and mechanical performance to evaluate their potential application in food packaging.

2. Materials and Methods

2.1. Materials

RS was obtained as waste of the rice industry that was collected in L'Albufera field (Valencia, Spain). It was supplied by the "Banco de Paja" (Valencia, Spain). The as-received

fibers were dried under vacuum (50 ± 2 °C, 0.5 mmbar) for 16 h and milled (3 cycles of 90 s each, IKA, model M20, Staufen, Germany), and sieved to <0.5 mm particle size.

Corn starch was supplied by Roquette (Roquette Laisa, Benifaió, Spain). Glycerol, magnesium nitrate ($\text{Mg}(\text{NO}_3)_2$), phosphorus pentoxide (P_2O_5), dimethyl sulfoxide (DMSO), methanol, and acetic acid were all obtained from Panreac Quimica S.L.U. (Castellar del Vallés, Barcelona, Spain). Sodium acetate trihydrate was purchased by Fluka™ (Steinheim, Germany). Sodium chlorite and heptane were provided by Sigma-Aldrich S.A. (Madrid, Spain).

2.2. Extraction of Cellulose Microfiber

A combination of ultrasound and heating treatments are known to lead to a certain degree of leaching out of hemicellulose and lignin present into the lignocellulosic RS matrix [8]. Based on this, CMFs were extracted according to our previous methodology [35]. Briefly, an aqueous dispersion of RS particles with 5% (w/v) solids was sonicated for 30 min at 25 °C (maintaining the temperature in an ice bath) using an ultrasonic homogenizer (750 W power, 20 kHz frequency, continuous mode) equipped with a high-intensity probe (Vibra Cell™ VCX750, Sonics & Material, Newton, MA, USA). After sonication, the RS dispersion was heated in a reflux heating apparatus at 100 °C for 1 h. Then, the plant dispersion was filtered using a qualitative filter (Filter Lab, Vidra Foc, Barcelona, Spain) and the solid fraction was dried at 40 °C for 48 h. Afterwards, the bleaching step of the cellulosic material was carried out by mixing the dry powder residue and the bleaching solution at 5% (w/v). The bleaching solution consisted of equal parts of sodium hypochlorite solution (1.7%, w/v), acetate buffer solution (2 N), and distilled water. The dispersion was treated under reflux heating for 4 cycles of 4 h each. The supernatant was filtered and the residue was washed with distilled water several times to remove the residual bleach solution at each stage. Then, the bleached solid fraction was dried at 35 °C for 48 h and milled using a milling machine (pulses of 2 s for 20 min, model M20, IKA Werke GmbH & Co. KG, Staufen, Germany) to obtain the so-called CMFs.

2.3. Dry Heating Treatment

Prior to melt mixing, corn starch was submitted to a DH pre-treatment, according to Maniglia et al. [33]. To this end, 50 g of starch were spread (1 mm thick layer) and compacted in an aluminum foil envelope. Then, the packaged sample was heated in a hot air oven (J.P. Selecta, S.A., Barcelona, Spain) at 130 °C for 4 h. Thereafter, the resultant starch was placed in a dark bottle and stored in a desiccator containing P_2O_5 at 6 ± 2 °C until further use.

2.4. Film Preparation

TPS and TPSDH films were prepared by melt blending and subsequent compression molding using glycerol as plasticizer 30 wt% with respect to the total starch mass. Green composites were obtained by addition of CMFs in concentrations of 1, 3, and 5 wt% in relation to the starch content based on the optimization performed in our previous study [36]. Table 1 summarizes the different sample compositions used to produce the films. The film components were previously dry mixed in a beaker and then melt-blended using an internal mini-mixer (HAAKETM PolyLab™ QC, Thermo Fisher Scientific, Karlsruhe, Germany) at 130 °C and 50 rpm for 10 min. The obtained dough was cold milled in the IKA's model and pre-conditioned at 25 °C and 53% RH using an $\text{Mg}(\text{NO}_3)_2$ over-saturated solution for one week.

The obtained doughs were compression molded to yield films in a hydraulic press (Model LP20, Labtech Engineering, Samut Prakan, Thailand). To this end, approximately 4 g of each dough was placed between two Teflon sheets and compressed in the hot plates. Control films (TPS) and those incorporating 1 wt% (TPS1), 3 wt% (TPS3), and 5 wt% (TPS5) of CMFs were preheated for 3 min at 160 °C in the plate press, then compressed at 160 °C for 2 min at 50 bars, followed by a second compression at 160 °C for 4 min at 130 bars,

and finally cooled down to 80 °C. The processing conditions of the films obtained using modified DH starch with CMFs (1 wt%: TPSDH1, 3 wt%: TPSDH3, and 5 wt%: TPSDH5) or without CMFs (TPSDH) were set as follows: preheating at 150 °C for 5 min, compression at 30 bars and 150 °C for 2 min, followed by 130 bars for 6 min, and then, final cooling to 80 °C. All films were conditioned at 25 °C and 53% RH ($\text{Mg}(\text{NO}_3)_2$) for one week before characterizations.

Table 1. Summary of compositions according to the mass fraction (g/g) of thermoplastic corn starch (TPS), thermoplastic dry heated corn starch (TPSDH), glycerol (Gly), and cellulose microfibril (CMF).

Sample	X_s	X_{Gly}	X_{CMF}
TPS	0.770	0.230	-
TPS1	0.763	0.229	0.008
TPS3	0.753	0.225	0.022
TPS5	0.741	0.222	0.037
TPSDH	0.770	0.230	-
TPSDH1	0.763	0.229	0.008
TPSDH3	0.753	0.225	0.022
TPSDH5	0.741	0.222	0.037

2.5. Material Characterization

2.5.1. Microscopy

An optical microscope (Optika Microscope B-350, OPTIKA S.r.l., Ponteranica, Italy) equipped with a camera (Optikam B2) was used to evaluate the morphology of the untreated RS and the resultant CMF samples before and after the milling process. To this end, the samples were extended with a water drop on the holder glass plate and the images were taken at 10× and 40× magnification. Morphogeometric properties of CMFs, expressed as cumulative distributions, were obtained by measuring the particle length (l) in different regions of the sample, as shown in the imaging procedure of Figure 1. The Optika Vision Lite program was used to obtain a minimum of 60 measurements.

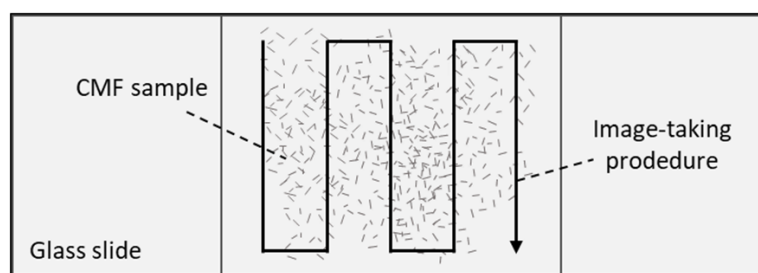


Figure 1. Image acquisition procedure to obtain the lengths of the cellulose microfibrils (CMFs).

The morphologies of RS, CMFs, and the cross-sections of the cryo-fractured films obtained by immersion in liquid nitrogen were evaluated using a Field Emission Scanning Electron Microscope (FESEM) equipped with focused ion gun (AURIGA Compact, Zeiss, Oxford Instruments). The conditioned samples (P_2O_5 at 25 ± 2 °C for 1 week) were covered with a platinum layer (EM MED020 sputter coater, Leica Biosystems, Barcelona, Spain), and the images were taken at 2.0 kV acceleration voltage. The SmartTiff program (version 2, Zeiss, Oxford Instruments, Abingdon, UK) was used to measure the particle width (w) a minimum of 60 times.

2.5.2. Optical Evaluation

Optical properties of the films were obtained according the Kubelka–Munk theory of multiple scattering to determine the film reflection spectra (R) using the black (R_0) and white (R_∞) backgrounds. The internal transmittance (T_i) of the films ranging from 400 to

700 nm, the film color coordinates L^* (lightness), a^* (redness-greenness), and b^* (yellowness-blueness) were determined using Equations (1)–(3), respectively. The colorimetric and transparency properties of the films were also evaluated in terms of hue angle (h_{ab}^*) (Equation (4)), chroma (C_{ab}^*) (Equation (5)), opacity (O) (Equation (6)), and total color difference (ΔE^*) (Equation (7)). The measurements were performed in triplicate.

$$T_i = \sqrt{(a + R_0)^2 - b^2} \quad (1)$$

$$a = \frac{1}{2} \left[R + \left(\frac{R_0 - R + R_g}{R_0 \times R_g} \right) \right] \quad (2)$$

$$b = \sqrt{a^2 - 1} \quad (3)$$

$$h_{ab}^* = \arctg\left(\frac{b^*}{a^*}\right) \quad (4)$$

$$C_{ab}^* = \sqrt{a^{*2} + b^{*2}} \quad (5)$$

$$O = A_{500} \times l \quad (6)$$

In which A_{500} and l are the absorbance at 500 nm and the film thickness, respectively.

$$\Delta E^* = \sqrt{(\Delta L^*)^2 + (\Delta a^*)^2 + (\Delta b^*)^2} \quad (7)$$

where $\Delta L^* = (L^* - L_0^*)$; $\Delta a^* = (a^* - a_0^*)$; $\Delta b^* = (b^* - b_0^*)$; and L_0^* , a_0^* , and b_0^* are the color coordinates of the control TPS film without fibers. The color differences were evaluated according to the following criteria [37]: $\Delta E^* < 1$ indicate unnoticeable color change; $1 \leq \Delta E^* \leq 2$ suggests that only an experienced observer can notice the difference; $2 \leq \Delta E^* \leq 3.5$ means that an inexperienced observer notices the difference; $3.5 \leq \Delta E^* \leq 5$ indicate clear noticeable difference; and $\Delta E^* \geq 5$ suggests that the observer notices different colors.

2.5.3. Equilibrium Moisture Content

The equilibrium moisture content of the films was determined by a gravimetric method. For this, film samples sizing 3 cm \times 3 cm that were previously conditioned (25 °C and 53% RH for two weeks) were dried at 60 °C for 24 h using a drying oven. Thereafter, the dried samples were placed in a desiccator containing P_2O_5 at 25 °C for two weeks to eliminate bonded water. Moisture content was determined from the total mass loss of the conditioned film during the drying process. The measurements were carried out in triplicate.

2.5.4. Water Solubility

Water solubility was determined based on the Talón et al. [38] methodology. A known mass of dry film sample (2 cm \times 2 cm), conditioned in P_2O_5 , were placed on a mesh, and immersed in a crucible with distilled water at 25 °C for 24 h. Afterwards, the sample-containing system was dried in an oven (J.P. Selecta, S.A.) at 60 °C for 48 h and, afterwards, conditioned in a desiccator with P_2O_5 at 25 °C for 1 week. The mass of residual film was weighed and compared with the initial mass of dry film. The measurements were carried out in triplicate and the results were expressed as g of solubilized film per 100 g film.

2.5.5. Barrier Measurements

Water vapor permeability (WVP) of the films was determined according to ASTM E96/E96M (ASTM, 2005) gravimetric methodology following the modifications proposed by McHUGH [39]. Film samples ($\varnothing = 3.5$ cm) were placed and sealed in Payne permeability cups filled with 5 mL of distilled water (100% RH). Then, the cups were placed into desiccators containing $Mg(NO_3)_2$ over-saturated solution (53% RH) and weighed periodically (ME36S, Sartorius, ± 0.00001 g, Fisher Scientific, Hampton, NH, USA) every

1.5 h for 25 h. For each treatment, the WVP was calculated considering the water vapor transmission rate (WVTR), which was determined from the slope of the weight loss vs. time. The measurements were performed in triplicate.

Oxygen permeability (OP) of the films was determined using an Ox-Tran equipment (Model 1/50, Mocon, Minneapolis, MN, USA) at 25 °C and 53% of RH, according to ASTM D3985-05 (ASTM, 2010). The used area of films was 50 cm² and the oxygen transmission rate (OTR) was obtained every 15 min until equilibrium was reached. The measurements were carried out in triplicate.

2.5.6. Mechanical Characterization

The tensile properties of the films were obtained according to ASTM D882 (ASTM, 2012). A universal testing machine (Stable Micro Systems, TA.XT plus, Stable Micro Systems, Godalming, UK) was used to determine elongation at break (EB), tensile strength at break (TS), and elastic modulus (EM). Film samples with dimensions of 25 mm × 10 mm were grabbed by two grips initially separated by 50 mm and stretched at a crosshead speed of 50 mm.min⁻¹. Eight samples were evaluated for each formulation. Before the analysis, the films were conditioned at 53% RH (Mg(NO₃)₂) and 25 °C for two weeks.

2.5.7. Thermal Analysis

The thermal stability of the films was determined by thermogravimetric analysis (TGA) using a thermogravimetric analyzer (TGA 1 Star^e System analyzer, Mettler-Toledo GmbH, Greifensee, Switzerland). Film samples, with a weight of 3–5 mg, were heated from 25 to 600 °C at a heating rate of 20 °C.min⁻¹ under nitrogen atmosphere (10 mL/min). For each thermal event, the initial (T_{onset}) and final (T_{final}) degradation temperatures, temperature of maximum degradation rate (T_{peak}), and the residual mass were determined by analyzing the TGA curves and their first derivative thermogravimetry (DTG) curves. The measurements were carried out in triplicate.

The phase transitions of the samples were investigated by differential scanning calorimeter (DSC) according to the method described by Collazo-Bigliardi et al. [40] with a DSC 1 Star^e System analyzer (Mettler-Toledo GmbH) operating under a nitrogen atmosphere (10 mL.min⁻¹). Samples of about 5–6 mg were weighted in aluminum pans and heated from 25 to 160 °C, cooled to 25 °C, and then heated (second heating step) to 160 °C at 10 °C.min⁻¹ using, in all cases, rates of 10 °C/min.

2.6. Statistical Analysis

The experimental data were submitted to multifactorial analysis of variance (ANOVA) at a confidence level of 95% using Minitab Statistical Program (version 17). Tukey's studentized range (HSD) test, considering the least significant difference of 5%, was applied to determine the influence of CMFs on the properties of the starch-based films.

3. Results

3.1. Morphological Characterization of CMFs

Figure 2 shows the FESEM micrographs of the untreated ground RS, the lignocellulosic residue after the combined ultrasound-heating treatment, the bleached cellulose fibers, and the resultant CMFs obtained after the milling step. It can be observed that the untreated RS (Figure 2a) presented heterogeneous particle sizes, with a predominance of rod-like shape, as seen in the magnified FESEM image. The RS particles showed mean sizes of width and length in the 20–60 µm and 16–270 µm ranges, respectively. Prior to the RS fiber extraction, the grinding step was applied to improve the effectiveness of the combined ultrasound-heating method and the bleaching treatment. According to Chen et al. [2], RS has a strong crystalline structure, making the extraction and purification of cellulose fibers difficult. Likewise, RS presents a high proportion of non-fibrous cells, such as parenchyma, epidermis, and vessel cells [41]. The traditional alkaline pre-treatment, which aims to eliminate hemicellulose and lignin [42], was replaced by a more environmentally friendly

aqueous treatment based on the application of ultrasound, followed by reflux heating. Figure 2b reveals that the application of ultrasound and heating promoted a certain degree of fibrillar plane de-bonding and distorted the RS particles, as previously reported [8]. The acoustic cavitation produced by the ultrasound waves, combined with the thermal erosion generated by reflux heating, promoted the disruption of the primary structure of RS and improved the leaching out of non-cellulosic components from the cellulosic matrix [43–45].

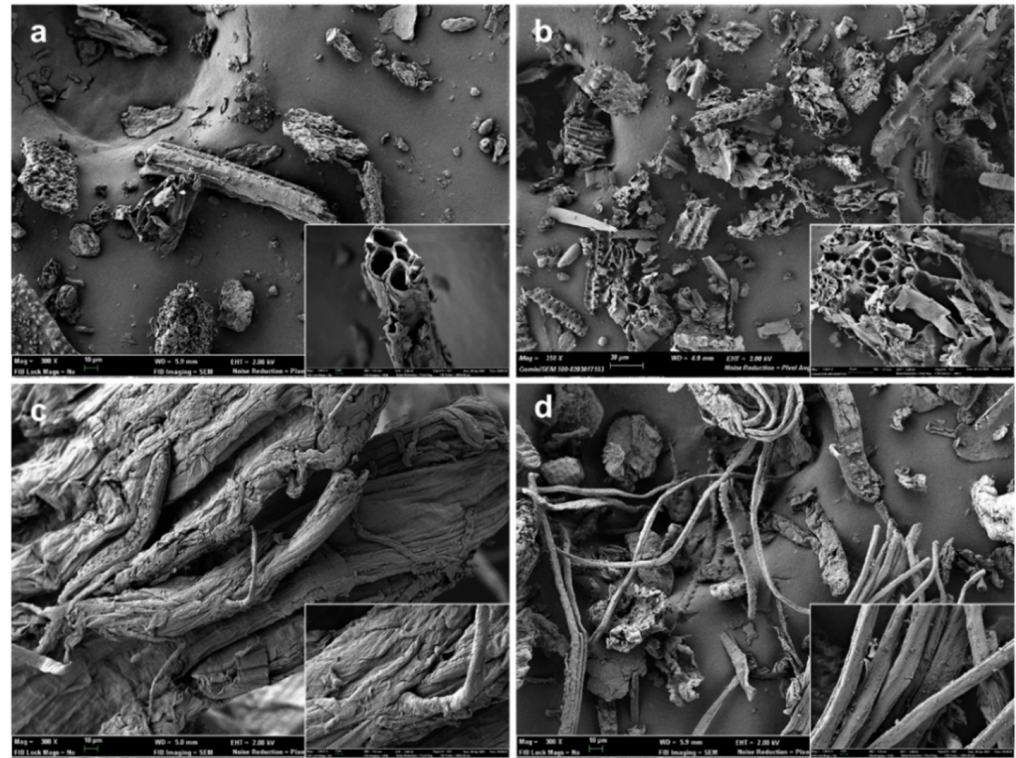


Figure 2. Field emission scanning electron microscope (FESEM) micrographs of untreated rice straw (RS) (a), RS treated with combined ultrasound-heating method (b), bleached cellulose microfibrils (CMFs) before (c) and after (d) the milling step. Images were taken at 300 \times with insets at 2000 \times .

As shown in Figure 2c, the bleached cellulose fibers exhibited a swollen, rough, and unregular appearance. The removal of non-fibrous components from the lignocellulosic matrix, such as hemicellulose, lignin, and waxes, gave rise to an entangled material, as observed by other authors [46]. The lignocellulosic matrix comprises cellulose fibrils organized in fibers arranged in a longitudinal orientation and inserted in a cementing matrix consisting of hemicellulose and lignin [2]. Thus, after removing the amorphous components, the hydroxyl (-OH) groups of cellulose could establish extensive hydrogen (-H) bonds among their chains, leading to a more compact and disordered arrangement [47]. This phenomenon can be observed in Figure 2c in the FESEM image taken at higher magnification. Thereafter, the cellulose fibers were ground to break up the agglomerates and obtain thinner CMFs (Figure 2d). Image analysis using both optical microscopy and FESEM techniques served to determine the cumulative distributions of CMF lengths and widths, respectively shown in Figure 3. Therefore, the mechanical defibrillation of the cellulose fiber bundles was evident, which was considered to occur by detaching CMFs into long fibrils with a major cumulative frequency of lengths below 200 μm (Figure 3a). Likewise, there was a marked reduction in the CMF thickness, showing predominant values between 5–15 μm . The magnified image of the ground material, shown in Figure 2d, revealed that CMFs were isolated with a smooth surface pattern, confirming that the milling step was an efficient method to disrupt the tangled microfibril arrangement. In this regard, Jiang et al. [48] observed that mechanical defibrillation was effective at detaching cellulose fibrils from RS treated with the 2,2,6,6-tetramethylpiperidine-1-oxyl (TEMPO)-

mediated oxidation method. The authors reported less uniform defibrillated particles, as also detected herein in Figure 2d. In this sense, the micrographs suggested that, due to the detachment of the fiber bundles into CMFs, the cellulosic material obtained could promote an efficient force transferring from the microfibers to polymer matrices, such as TPS [49].

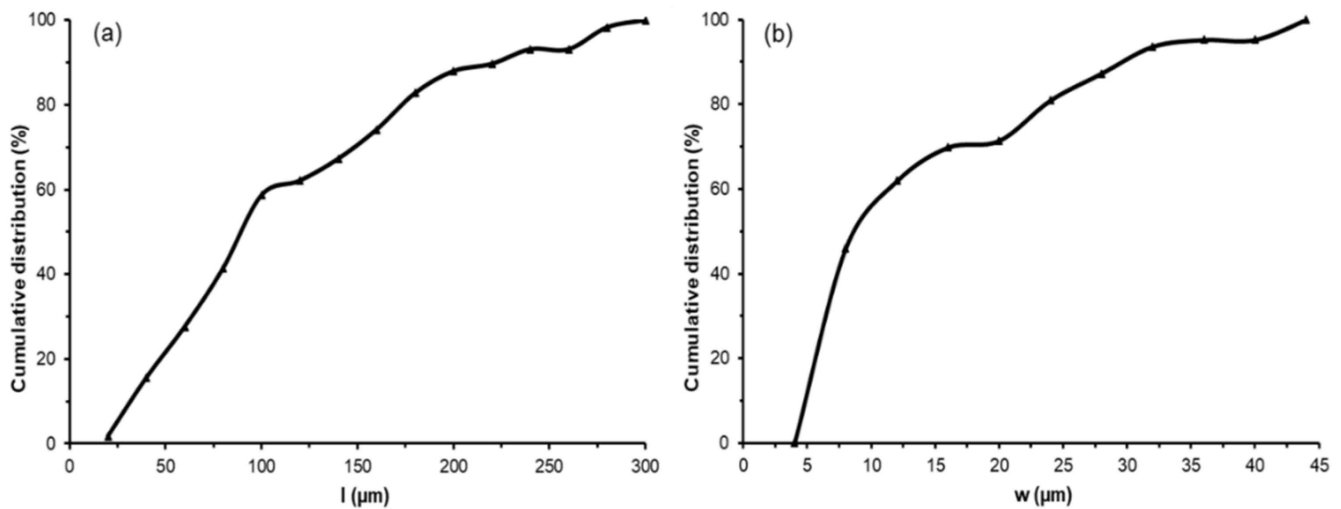


Figure 3. Cumulative distributions of cellulose microfiber (CMF) length (l) (a) and width (w) (b) obtained from image analyses of optical microscopy and field emission scanning electron microscopy (FESEM), respectively. A minimum of 60 measurements for each parameter was performed.

3.2. Microstructure of the Films

Figure 4 shows the FESEM micrographs of the cross-sections of the TPS-based films incorporating different CMF concentrations (1, 3, and 5 wt%) obtained by cryo-fracture and their corresponding samples using DH-modified starch, that is, TPSDH. The TPS control film samples revealed a smooth and homogeneous cross-section surface pattern, indicating a good starch thermoplasticization, as also reported by other authors for starch films obtained in similar conditions [50,51]. In contrast, the TPSDH films exhibited remaining starch granules, which suggests changes in the starch thermoplasticization behavior after the DH treatment. In this context, Chandanasree et al. [31] reported that the treatment of native starch by DH provokes partial damages in the semi-crystalline and crystalline regions of the granules, which prevent the granule swelling and delays its gelatinization. Furthermore, the DH treatment can oxidize and convert the -OH groups present in the starch chains to carbonyl (C=O) and carboxyl (-COOH) groups, which alters the gelatinization profile [52]. A progressive increase in the number of non-gelatinized starch granules was also observed in the cross-sections of the films of non-modified starch when the CMF concentration increased. However, this number increased in the samples prepared with DH-modified starch.

The starch thermoplasticization occurs during heating, in the extruder or melt-mixing equipment, in the presence of a plasticizer, such as glycerol, at high temperatures (130 °C) and pressures [21]. The microstructural features of the microcomposite films revealed that the CMF incorporation interfered the starch gelatinization with glycerol. This could be explained by the competitive interaction of the plasticizer with both CMFs and starch through -H intermolecular bonds with the cellulose chains, decreasing their availability and subsequently provoking gelatinization of the granular structure of starch. This effect was mainly observed in the TPSDH samples, where the thermal treatment involved changes in its granular structure that already limits its gelatinization.

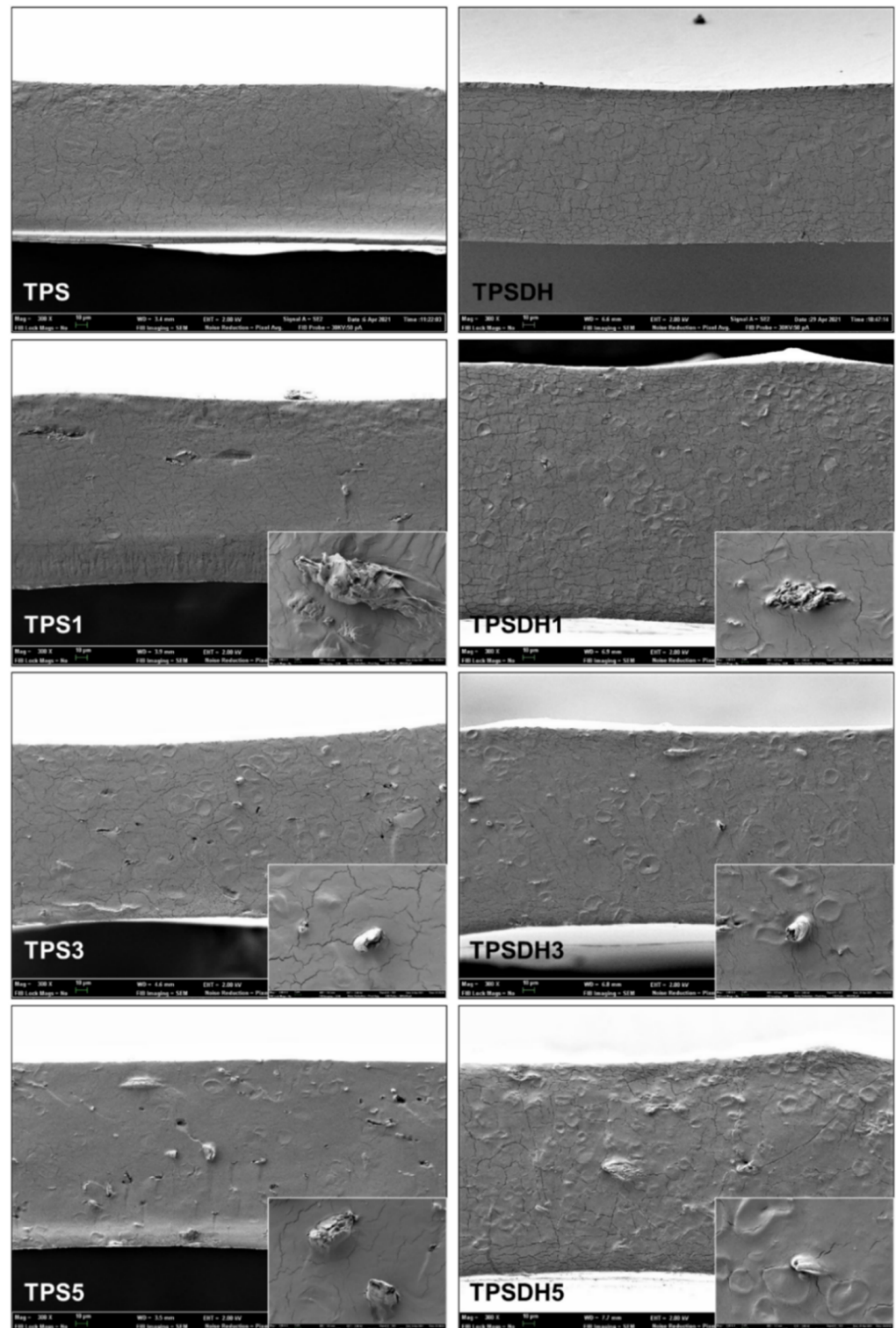


Figure 4. Field emission scanning electron microscope (FESEM) micrographs of the fracture surfaces of thermoplastic starch (TPS) and TPS modified by dry heating (TPSDH) films with contents of cellulose microfibrils (CMFs) of 1 wt% (TPS1, TPSDH1), 3 wt% (TPS3, TPSDH3), and 5 wt% (TPS5, TPSDH5). Images were taken at 300 \times with insets at 2000 \times .

Figure 4, which shows the fracture surfaces of film samples, revealed that the CMFs incorporated into the films exhibited good compatibility with both types of TPS matrices, that is, non-modified and DH-modified starch. This observation can be deduced from the good interfacial adhesion observed between the fibers and starch matrix due to the absence

of gap between the fiber surface and the TPS matrix. Nevertheless, the film cryo-fracture does not seem to promote the breakage of the fibers, but their separation from the matrix, resulting in hollows that arise from the outgoing fiber during the fracture of the film samples. Similar findings were observed by Collazo-Bigliardi et al. [40] and Kargarzadeh et al. [28] in TPS films reinforced with CMFs from rice husk. The apparently good interfacial adhesion properties of fibers in the starch matrices could derive from the obtaining process of CMFs, without alkaline pre-treatment, which promoted the presence of exposed -OH groups on the surface of the fibers [53], thus enhancing the -H bond interactions with the -OH groups of starch.

3.3. Optical Properties: Color and Transparency

Film color and transparency are not only important factors in food packaging designs, but also very useful for evaluating the filler-polymer matrix compatibility. Table 2 summarizes the color coordinates in terms of L^* , C_{ab}^* , and h_{ab}^* as well as the total color difference (ΔE^*) with respect to the neat TPS films without DH treatment and CMFs and the opacity coefficient of the different films. Likewise, the T_i spectra of the different films are shown in Figure 5. Both the CMF incorporation and starch DH modification significantly ($p < 0.05$) affected the evaluated optical properties. Comparison of TPS and TPSDH films without fibers permits to elucidate that DH gave rise to slightly darker films with more saturated, that is, higher C_{ab}^* values, and a yellower color, which suggest that Maillard or sugar caramelization reactions could occur during thermal treatment of native starch. Likewise, as the CMF concentration increased, both TPS and TPSDH films exhibited a slight decrease in their lightness (L^*) while color saturation (C_{ab}^*) increased and hue tended to be more yellowish. This was reflected on the ΔE^* values, in which the color coordinates L^* , a^* , and b^* of the TPS control film were used as a reference. In the TPS films without DH treatment, the ΔE^* values attained after the incorporation of low contents of CMFs were below 1 indicating unnoticeable color changes, whereas only in the microcomposite with 5 wt% CMFs, that is, TPS5, an unexperienced observer can already observe color differences ($2 \leq \Delta E^* \leq 3.5$). In the TPSDH films, as opposite, the combined effect of dispersed phases, that is, CMFs and non-gelatinized starch granules, and colored compounds formed during thermal modification of starch [31,54], gave rise to higher color variations with respect to the neat TPS films. Thus, the TPSDH and its microcomposite with the lowest CMF content showed clear noticeable differences ($3.5 \leq \Delta E^* \leq 5$), whereas the samples with higher fiber contents yielded films with a noticeable different color ($\Delta E^* \geq 5$).

Table 2. Optical properties in terms of lightness (L^*), chroma (C_{ab}^*), hue angle (h_{ab}^*), color difference (ΔE^*), and opacity (O) of thermoplastic starch (TPS) and TPS modified by dry heating (TPSDH) films with different contents of cellulose microfibrils (CMFs).

Formulation	L^*	C_{ab}^*	h_{ab}^*	ΔE^*	O
TPS	88.5 ± 0.1 ^{a,1}	7.6 ± 0.1 ^{f,2}	92.6 ± 0.1 ^{a,1}	-	0.141 ± 0.001 ^{b,2}
TPS1	88.5 ± 0.1 ^{a,3}	7.5 ± 0.2 ^{f,2}	92.8 ± 0.1 ^{a,1}	0.07 ± 0.01 ^e	0.146 ± 0.009 ^{b,2}
TPS3	88.1 ± 0.2 ^{b,5}	8.2 ± 0.3 ^{e,2}	92.6 ± 0.2 ^{a,1}	0.70 ± 0.02 ^e	0.151 ± 0.005 ^{ab,2}
TPS5	87.6 ± 0.2 ^{c,7}	9.4 ± 0.3 ^{d,2}	91.5 ± 0.2 ^{b,1}	2.03 ± 0.01 ^d	0.140 ± 0.005 ^{b,2}
TPSDH	86.0 ± 0.1 ^{d,2}	11.9 ± 0.5 ^{c,1}	89.2 ± 0.2 ^{cd,2}	4.76 ± 0.05 ^c	0.163 ± 0.001 ^{ab,1}
TPSDH1	86.2 ± 0.2 ^{d,4}	11.3 ± 0.2 ^{c,1}	89.5 ± 0.3 ^{c,2}	4.64 ± 0.10 ^c	0.163 ± 0.006 ^{ab,1}
TPSDH3	85.4 ± 0.1 ^{e,6}	12.4 ± 0.2 ^{b,1}	88.9 ± 0.1 ^{d,2}	6.24 ± 0.01 ^b	0.171 ± 0.007 ^{a,1}
TPSDH5	84.5 ± 0.1 ^{f,8}	14.2 ± 0.2 ^{a,1}	88.8 ± 0.1 ^{d,2}	7.88 ± 0.15 ^a	0.156 ± 0.007 ^{ab,1}

Different subscript letters indicate significant differences between samples of the same group (TPS or TPSDH films). Different numbers indicated significant differences between TPS and TPSDH samples with the same ratio of CMF (Tukey test, $p < 0.05$).

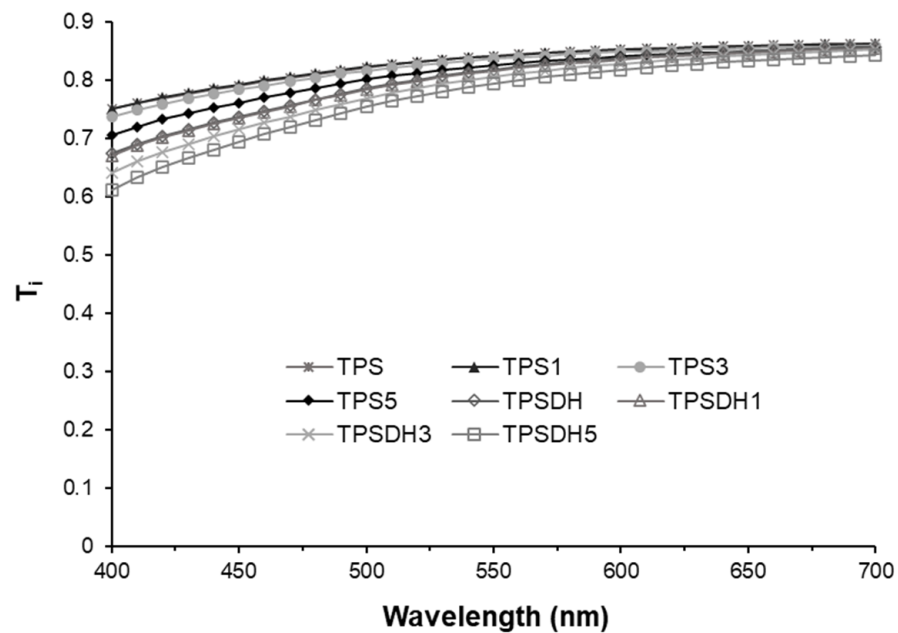


Figure 5. Internal transmittance (T_i) of thermoplastic starch (TPS) and TPS modified by dry heating (TPSDH) films with different contents of cellulose microfibers (CMFs).

The T_i spectra of the films within the wavelength range of 400–700 nm shown in Figure 5 revealed that the TPSDH films without CMFs exhibited lower transparency than the TPS films, with lower values of T_i , mainly at the lowest wavelength. This can be explained by the presence of colored compounds, formed during the starch DH modification process and the presence of dispersed starch granules in the films, which were non-completely gelatinized. These dispersed particles, having refractive indexes different from that of the starch continuous phase, promoted light scattering and film opacity. In both kinds of films, a slight and progressive decrease in light transmission was observed as the CMF concentration increased. This result agrees with the observations reported by other authors for CMF-containing TPS samples [36,55,56], where the filler incorporation as dispersed phase also caused changes in the refractive index of the polymer matrix, promoting light scattering and opacity in the films. Therefore, opacity increased due to the presence of CMFs and the non-gelatinized starch granules. In particular, the opacity parameter, also included in Table 2, increased from 0.141 for the neat TPS film up to 0.171 for the TPSDH3 film.

3.4. Equilibrium Moisture Content and Water Solubility

Table 3 shows the equilibrium moisture content and water solubility of the different films prepared with TPS and TPSDH. One can observe that the DH treatment of starch slightly promoted water sorption capacity and water solubility of the films. In this sense, Lim et al. [57] reported that DH treatment of starch can damage its granular structure, which culminates in the exposure of its -OH groups, promoting the ability to interact with water molecules and water sorption capacity. Oh et al. [32] also reported an increase in water solubility of rice starch modified with the DH treatment. Furthermore, the CMF incorporation slightly decreased the water sorption capacity of both TPS and TPSDH films, whereas it provided different effects on water solubility for each kind of starch film, reducing solubility for the TPS films but increasing it in the case of the TPSDH films. The small changes in the water sorption capacity provoked by CMFs can be explained in terms of the lower water affinity of the fibers in comparison with TPS [58], reflected on their low equilibrium water content (3%) at 53% RH [35]. In fact, the resulting water content of the microcomposites could be deduced from the mass balance considering the equilibrium water content of both starch matrix and fibers.

Table 3. Moisture, water solubility, water vapor permeability (WVP), and oxygen permeability (OP) of thermoplastic starch (TPS) and TPS modified by dry heating (TPSDH) films with different contents of cellulose microfibrils (CMFs).

Formulation	Moisture (%)	Solubility (g Soluble Film·100 g ⁻¹ Film)	WVP (g·mm·kPa ⁻¹ ·h ⁻¹ ·m ⁻²)	OP × 10 ¹⁴ (cm ³ ·m ⁻¹ ·s ⁻¹ ·Pa ⁻¹)
TPS	7.7 ± 0.1 ^{a,1}	42 ± 2 ^{a,2}	6.3 ± 0.2 ^{a,b,1}	9.0 ± 0.3 ^{a,1}
TPS1	7.5 ± 0.1 ^{a,1}	28 ± 1 ^{b,2}	6.5 ± 0.1 ^{a,1}	9.2 ± 0.4 ^{a,1}
TPS3	7.7 ± 0.1 ^{a,1}	37 ± 4 ^{ab,2}	5.9 ± 0.2 ^{b,1}	6.3 ± 0.6 ^{b,2}
TPS5	7.1 ± 0.2 ^{b,1}	36 ± 5 ^{ab,2}	5.3 ± 0.3 ^{c,1}	6.4 ± 0.1 ^{b,2}
TPSDH	8.1 ± 0.1 ^{a,2}	55 ± 8 ^{b,1}	0.25 ± 0.01 ^{a,2}	8.7 ± 0.5 ^{a,1}
TPSDH1	7.9 ± 0.1 ^{a,2}	80 ± 8 ^{a,1}	0.33 ± 0.05 ^{a,2}	8.8 ± 0.4 ^{a,1}
TPSDH3	7.7 ± 0.1 ^{b,1}	73 ± 12 ^{ab,1}	0.31 ± 0.02 ^{a,2}	7.7 ± 0.4 ^{a,1}
TPSDH5	7.9 ± 0.1 ^{a,2}	57 ± 6 ^{ab,1}	0.31 ± 0.01 ^{a,2}	8.4 ± 0.1 ^{a,1}

Different subscript letters indicate significant differences between samples of the same group (TPS or TPSDH films). Different numbers indicated significant differences between TPS and TPSDH samples with the same ratio of CMF (Tukey test, $p < 0.05$).

The different effect of the fibers on water solubility of TPS and TPSDH films can be explained by the different interactions of CMFs with both starch matrices. The -OH groups present in CMFs could interact with the hydrophilic groups in starch, making it unavailable to interact with the water molecules [59]. This effect was evident for the water solubility of the TPS films, which decreased significantly ($p < 0.05$) after the CMF incorporation, as previously reported by other authors [56,60,61]. Furthermore, the lower water solubility of these microcomposites due to the CMF presence could make starch less susceptible to hydrolysis, though this property mainly depends on its structural characteristics and modifications [62]. However, in the TPSDH films, the CMF incorporation promoted film water solubility, except for the samples containing 5 wt% CMFs. This different effect could be ascribed to a poorer integration and dispersion of the fibers in the starch matrix, having lower adhesion forces at the interface and, thus, favoring water penetration through the junction zones. The higher presence of non-gelatinized starch granules could also contribute to the higher solubility in the TPSDH films since this dispersed phase can reduce the cohesion forces of the matrix, which are related to the interchain bonds that depend on their interfacial adhesion in the continuous matrix.

3.5. Barrier Properties to Water Vapor and Oxygen Gas

The values of WVP and OP of the TPS films are also shown in Table 3. The non-modified starch films exhibited WVP values ranging from 5.3 to 6.3 g·mm/kPa·h·m², close to the range reported by other authors for corn starch films [34,40]. Films of TPS with 3 and 5 wt% CMFs exhibited slightly lower but still significant ($p < 0.05$) WVP values than the neat TPS film, reaching percentages increases in the barrier performance of 6% and 15%, respectively. Since WVP of packaging materials is mainly affected by the solubility coefficient in the polymer matrix and also, but to a lesser extent, by the vapor diffusion rate [63], the permeability decrease attained in the film samples containing CMFs can be ascribed to the chemical interaction by -H bonds of cellulose with hydrophilic groups of the starch-glycerol matrix described above [4,49,64]. Other authors also reported a decrease in WVP of TPS films from different sources incorporated with cellulosic fractions [61,65]. Furthermore, the CMF addition did not influence significantly ($p > 0.05$) the WVP values of the TPSDH films, which already presented values remarkably lower ($p < 0.05$) than the TPS samples. The latter lower permeability to water vapor of DH-modified starch can be ascribed to the large presence of intact starch granules, previously observed in the FESEM images, which would increase the tortuosity factor of the modified matrix, further limiting the diffusion of water molecules through the films. Other authors also reported lower values of WVP for DH-modified rice starch films [66].

As concerns the OP values, the incorporation of CMFs at contents of 3 and 5 wt% promoted a significant ($p < 0.05$) OP decrease of approximately 30% with respect to the neat TPS film. This barrier enhancement can be attributed to the increase of the tortuosity factor

associated with the fiber distribution along the TPS matrix, with a good compatibility and dispersion, which would limit the diffusion rate of oxygen molecules through the films. Other studies have also reported a decrease in the OP of starch-based films with cellulosic fractions [36,65], which are in agreement with the results reported herein. However, non-significant differences ($p > 0.05$) in the OP values were observed for the TPSDH films after fiber incorporation. These films exhibited significantly ($p < 0.05$) higher OP values than TPS microcomposite films with 3 and 5 wt% CMFs and similar to those observed for TPS films without and with 1 wt% CMFs. The lack of influence of the incorporated fibers on the barrier properties (both WVP and OP) of the TPSDH films suggests that the expected fiber promotion of the tortuosity factor is probably compensated by lower adhesion forces between the fibers and biopolymer matrix that promoted mass transfer through the union points. Moreover, the larger content of C=O and -COOH groups produced by depolymerization of heat-treated starch chains could promote the solubility of oxygen molecules in the films, enhancing the transmission rate [67].

Therefore, incorporating CMFs from RS in TPS films represents an adequate strategy to enhance the oxygen barrier capacity of the biopolymer films, being suitable to reduce or modulate oxidation reactions in packaged foods. In contrast, a very low effect of CMFs on the barrier properties of the DH-modified starch films was observed, though these biopolymer films already exhibited a better water vapor barrier capacity (90% reduction of WVP with respect to untreated TPS films).

3.6. Mechanical Properties

The mechanical properties of the films, namely EB, TS, and EM were determined by tensile tests and are summarized in Table 4. Both TPS and TPSDH films exhibited similar stiffness or elastic modulus, though the TPSDH films were slightly more rigid and remarkably more resistant to break but also less extensible. The TPS control film had an EB value of approximately 30%, in line with that observed by Hernández-García et al. [50] for TPS films. Furthermore, the TPSDH film without fibers showed an EB value of 23%, being lower than the neat TPS film. This mechanical embrittlement can be attributed to the changes occurred in the starch chains, such as short-chain amyloses produced by heat-induced hydrolysis of starch [54] or the increase in the content of C=O and -COOH groups during the DH of starch [67]. Other authors [60,68] also suggested that the conversion of native -OH groups to C=O and -COOH ones in oxidized starch may promote -H bonds between amylose and amylopectin molecules, increasing the integrity of the biopolymer matrix and improving the tensile resistance of the films.

Table 4. Mechanical properties in terms of elongation at break (EB%), tensile strength at break (TS), and elastic modulus (EM) of thermoplastic starch (TPS) and TPS modified by dry heating (TPSDH) films with different contents of cellulose microfibers (CMFs).

Formulation	EB (%)	TS (MPa)	EM (MPa)
TPS	30 ± 4 ^{a,1}	3.4 ± 0.6 ^{c,2}	180 ± 50 ^{c,1}
TPS1	30 ± 7 ^{a,1}	4.2 ± 1.0 ^{bc,2}	140 ± 30 ^{c,2}
TPS3	14 ± 5 ^{b,1}	6.8 ± 1.2 ^{a,2}	550 ± 180 ^{a,1}
TPS5	18 ± 4 ^{b,1}	4.6 ± 0.9 ^{b,2}	300 ± 100 ^{b,1}
TPSDH	23 ± 4 ^{a,2}	6.4 ± 0.4 ^{b,1}	190 ± 30 ^{f,1}
TPSDH1	9 ± 3 ^{bc,2}	6.9 ± 0.5 ^{b,1}	320 ± 70 ^{e,1}
TPSDH3	5 ± 1 ^{c,2}	10.2 ± 1.5 ^{a,1}	590 ± 70 ^{d,1}
TPSDH5	10 ± 3 ^{b,2}	7.2 ± 1.2 ^{b,1}	290 ± 100 ^{ef,1}

Different subscript letters indicate significant differences between samples of the same group (TPS or TPSDH films). Different numbers indicated significant differences between TPS and TPSDH samples with the same ratio of CMF (Tukey test, $p < 0.05$).

The incorporation of CMFs at 3 wt% increased notably film stiffness in both kinds of films, being this effect less noticeable at other ratios of fibers. Several studies have also reported higher EM values of starch films containing cellulosic fractions from different

sources [36,56,69]. In general, all the here-developed films became more resistant and less stretchable as higher loading of CMFs were incorporated. Higher fiber contents, of 3 and 5 wt% CMFs, decreased the TPS film stretchability by about 50%, whereas a similar decrease was observed for the TPSDH film with only 1 wt% CMFs. The lack of stretchability limits the overall extensibility of the films without markedly reducing the resistance to break. As shown in FESEM micrographs, CMFs were strongly bonded to the polymer matrix, which restricted the movement of starch chains, decreasing their stretchability but also reinforcing the TPS matrix [70]. The highest reinforcing effect was observed for the 3 wt% CMFs in both TPS and TPSDH films. These films particularly exhibited the highest EM (about 550 and 590 MPa for TPS and TPSDH, respectively) and resistance to break (approximately 7 and 10 MPa for TPS and TPSDH, respectively), but also with reduced elongation capacity (14 and 5% for TPS and TPSDH, respectively). In this regard, Fazeli et al. [65] also observed a threshold concentration in cellulose nanofibers from henequen to reinforce starch films.

Therefore, the obtained results in tensile behavior of TPS and TPSDH films demonstrated the reinforcing capacity of CMFs for starch films, which indicates good compatibility and dispersion along the TPS matrix. However, contents higher than 3 wt% led to lower mechanical performances, which can be attributed to a loss of cohesion forces or a lower degree of dispersion and certain agglomeration of the fibers in the TPS matrix.

3.7. Thermal Properties

Figure 6 shows the TGA and first derivative (DTG) curves obtained for the TPS and TPSDH films and their microcomposites films prepared with CMFs. Table 5 gathers the thermal stability parameters, namely T_{onset} , T_{final} , and T_{deg} as well as the mass loss at T_{deg} . One can observe that fiber incorporation did not notably influence the thermal degradation properties of the TPS and TPSDH films. In particular, the TPS films showed the main degradation event ranging at approximately 150–455 °C, corresponding to a mass loss of nearly 80% with a T_{deg} value of 341 °C. This event is associated with the thermal decomposition of glycerol [71], starch [28,72], and CMFs. Figure 6a shows the thermal decomposition profile of the CMF fractions, showing the previously reported mass loss steps [35]: evaporation of bonded water (30–140 °C), cellulose and hemicellulose decomposition (177–350 °C) and lignin degradation (350–500 °C). The second thermal degradation step is referred as the “active pyrolysis zone” since the mass loss rate is high, whereas the third one is called “passive pyrolysis zone” since the percentage of mass loss is smaller, and the mass loss rate is also much lower compared to that in the second zone [73]. In relation to the degradation profile of the TPS films, the sample containing 5 wt% CMFs exhibited slightly higher mass loss from 180 to 280 °C, which can be attributed to the thermal degradation of the cellulose fractions, more noticeable due to its high content. However, this TPS5 sample was more stable than the other TPS films in the thermal range of 280–310 °C (see Figure 6a,c), suggesting that the CMF incorporation delayed the thermal degradation of the shortest chains of starch produced during its thermo-processing [74].

Regarding the TPSDH films, these samples exhibited a slight initial mass loss (3–5%) in the thermal range from approximately 50 to 150 °C, which is ascribed to evaporation of water adsorbed in the inner regions of the non-gelatinized starch granules and it may also derive from thermal decomposition of low-molecular weight (M_w) components produced during the DH treatment [54]. This mass loss can be observed in Figure 6b, where the mass loss curves of the TPS and TPSDH films were compared. As shown in Table 4 and also Figure 6d, TPSDH films exhibited slightly higher T_{deg} values than the TPS films. This thermal stability enhancement may be attributed to the presence of C=O and -COOH groups produced by the heat treatment of starch that allows for more -H bonds between the polymer chains [68]. Furthermore, the non-gelatinized starch granules, with more crystalline regions, could also contribute to the resultant thermal behavior. In the TPSDH films, the concentration increases in CMFs also implied a slight increase in the thermal stability, which could be due to the increasing presence of starch granules in the matrix.

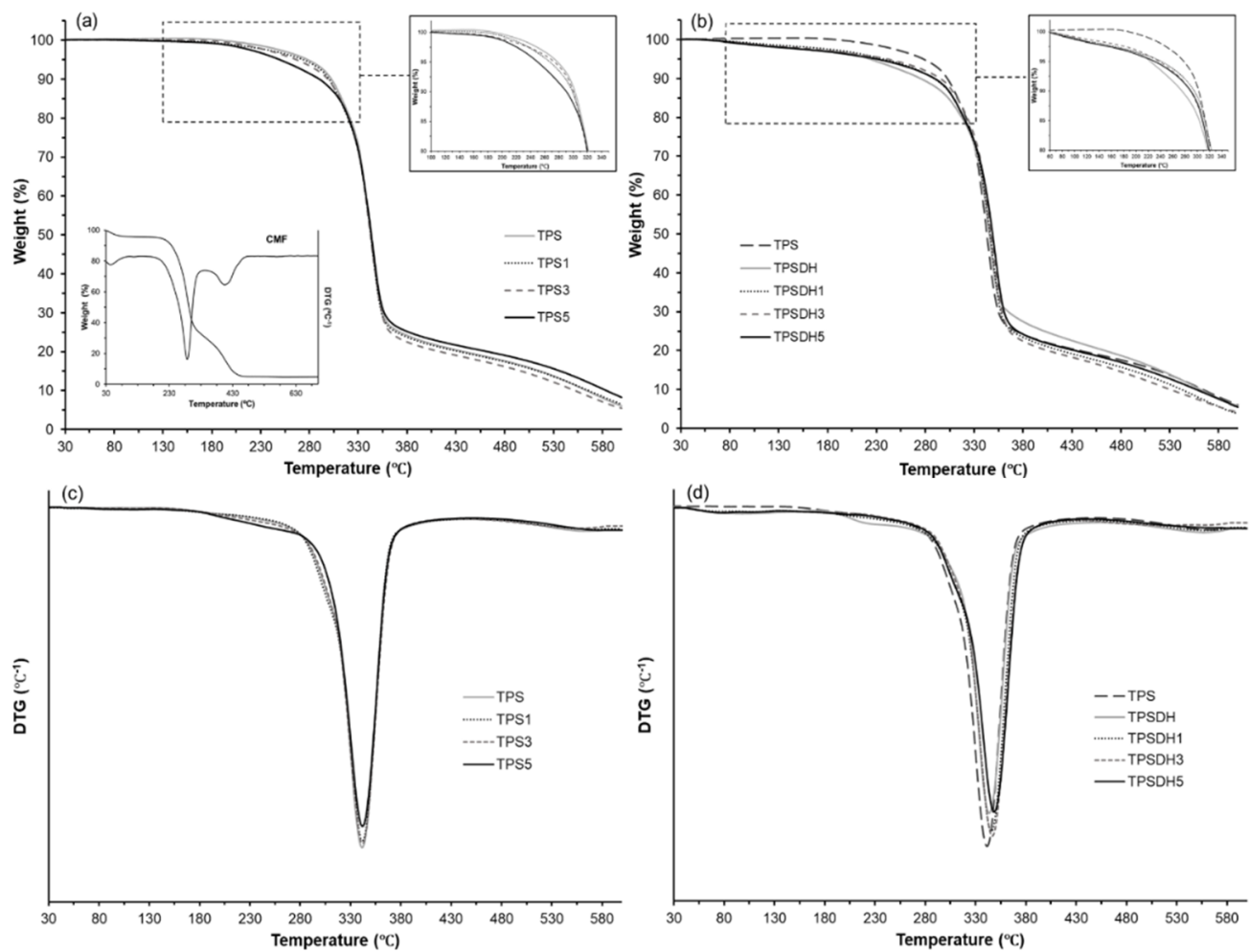


Figure 6. Thermogravimetric analysis (TGA) curves (a,b) and first derivative (DTG) curves (c,d) curves of thermoplastic starch (TPS) and TPS modified by dry heating (TPSDH) films with different contents of cellulose microfibers (CMFs).

Table 5. Onset, final, and peak temperatures (T_{onset} , T_{final} , and T_{deg}), and mass loss at T_{deg} ($\Delta m\%$) obtained from thermogravimetric analysis (TGA) and glass transition temperature (T_g) obtained from differential scanning calorimetry (DSC) for thermoplastic starch (TPS) and TPS modified by dry heating (TPSDH) films with different contents of cellulose microfibers (CMFs).

Formulation	TGA				DSC
	T_{onset} (°C)	T_{final} (°C)	T_{peak} (°C)	Δm (%)	T_g
TPS	156 ± 1	455 ± 3	341 ± 1	80.7 ± 1.0	92 ± 4
TPS1	153 ± 1	456 ± 1	343 ± 1	81.3 ± 0.7	86 ± 1
TPS3	152 ± 4	453 ± 1	342 ± 1	82 ± 1.0	85 ± 6
TPS5	154 ± 1	452 ± 3	343 ± 1	79.2 ± 0.2	82 ± 9
TPSDH	179 ± 2	455 ± 1	345 ± 1	80 ± 1	106 ± 1
TPSDH1	183 ± 1	454 ± 2	346 ± 2	78 ± 2	79 ± 2
TPSDH3	181 ± 1	449 ± 2	347 ± 1	80 ± 1	-
TPSDH5	182 ± 1	450 ± 1	349 ± 3	79 ± 3	124 ± 4

Finally, DSC analysis was also performed to evaluate the effect of the starch modification by DH and CMF incorporation on the thermal phase transitions of starch. The first heating scans, gathered in Figure 7, showed the typical endotherm of starch gelatinization associating peak temperatures in the 55–110 °C range for the film samples of TPSDH and TPS with the highest CMF loadings (TPS3 and TPS5). This agrees with the above-reported FESEM observations that revealed the presence of non-gelatinized starch granules in the

starch matrix. It can also be observed that the gelatinization enthalpy increased with the CMF ratio due to the aforementioned higher presence of starch granules in the films. In the second heating scan, the TPS films also exhibited the glass transition (T_g) of the already gelatinized starch, being this transition less appreciable, that is, having a lower change in specific heat (ΔC_p) for TPSDH samples. The T_g values (midpoint) of the TPSDH sample was slightly higher than that of TPS, which is coherent with the stronger interactions promoted in the matrix when starch was DH modified. This result also agrees with the more resistance but less ductile behavior of the films attained during the mechanical characterization. As expected, the addition of CMFs did not induce notable changes in the starch's T_g , when compared with the corresponding control sample, since the fibers are not miscible with starch. The small variations of T_g in the TPS composites with CMFs can be attributed to potential interactions between fibers or their remaining water contents and plasticizer that could modify the plasticization level of starch [31]. In this context, Collazo-Bigliardi et al. [40] found similar results for corn starch films filled with fibers derived from rice husk.

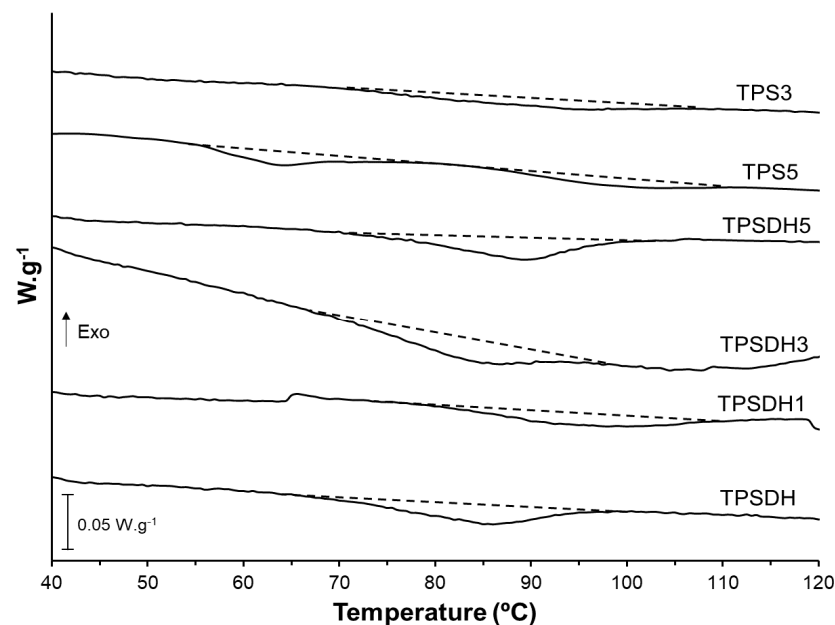


Figure 7. Differential scanning calorimetry (DSC) thermograms taken during first heating scan of thermoplastic starch (TPS) and TPS modified by dry heating (TPSDH) films with different contents of cellulose microfibrils (CMFs).

4. Conclusions

CMFs with good reinforcing capacity for starch films were obtained from RS, a waste material derived from the agricultural and food industry, using a green process and mechanical defibrillation. Fibrils with a major cumulative frequency of lengths below 200 μm and 5–15 μm of thickness were obtained. Incorporation of CMFs into starch matrices at 3 wt%, the most optimal content, led to stiffer and more resistance to break films for both non-modified and DH-modified corn starch films. Likewise, fibers at 3 and 5 wt% improved the oxygen and water vapor barrier capacity of TPS films but did not modify barrier properties of TPSDH films. Fibers interfered starch gelatinization during the starch–glycerol thermo-processing, more markedly in DH-modified starch with modified granular structure, giving rise to non-gelatinized starch granules into the film matrix. The dispersed phase (starch granules or fibers) also modified the optical properties of the TPS films, making them slightly less transparent. Therefore, it can be concluded that RS is a good source of CMFs that can be used to improve properties of starch films with different purposes, such as their use as food packaging material. This contributes to the valorization of the agricultural and food waste into added-value materials, useful for improving the

performance of biodegradable food packaging materials. Likewise, this study further confirms that the DH process of starch represents a green physical method to enhance the water barrier capacity and tensile strength of starch films. Future studies will deal with the hydrolysis resistance of these microcomposite films and their practical application as packaging materials in food preservation.

Author Contributions: P.A.V.F.: conceptualization, methodology, formal analysis, investigation, writing—original draft preparation, writing—review and editing; C.I.L.F.A.: conceptualization, methodology, formal analysis, investigation, data analysis; S.T.-G.: writing—original draft preparation, writing—review and editing; C.G.-M.: conceptualization, methodology, investigation, writing—original draft preparation, writing—review and editing; A.C.: conceptualization, methodology, investigation, writing—original draft preparation, writing—review and editing. All authors have read and agreed to the published version of the manuscript.

Funding: This research was funded by Spanish Ministry of Science and Innovation (MICI), grant number PID2019-105207RB-I00.

Institutional Review Board Statement: Not applicable.

Informed Consent Statement: Not applicable.

Acknowledgments: P.A.V.F. is grateful to Generalitat Valenciana (GVA) for the Grisolia P/2019/115 grant. C.I.L.F.A. acknowledges the São Paulo Research Foundation (FAPESP) for the Research Internships Abroad (BEPE) fellowship (2020/10498-0). S.T.-G. acknowledges MICI for his Ramón y Cajal contract (RYC2019-027784-I).

Conflicts of Interest: The authors declare no conflict of interest.

References

1. Hafemann, E.; Battisti, R.; Marangoni, C.; Machado, R.A.F. Valorization of Royal Palm Tree Agroindustrial Waste by Isolating Cellulose Nanocrystals. *Carbohydr. Polym.* **2019**, *218*, 188–198. [CrossRef]
2. Chen, X. Study on Structure and Thermal Stability Properties of Cellulose Fibers from Rice Straw. *Carbohydr. Polym.* **2011**, *85*, 245–250. [CrossRef]
3. Saini, J.K.; Saini, R.; Tewari, L. Lignocellulosic Agriculture Wastes as Biomass Feedstocks for Second-Generation Bioethanol Production: Concepts and Recent Developments. *3 Biotech.* **2015**, *5*, 337–353. [CrossRef] [PubMed]
4. Ng, H.-M.; Sin, L.T.; Tee, T.-T.; Bee, S.-T.; Hui, D.; Low, C.-Y.; Rahmat, A.R. Extraction of Cellulose Nanocrystals from Plant Sources for Application as Reinforcing Agent in Polymers. *Compos. Part B Eng.* **2015**, *75*, 176–200. [CrossRef]
5. Sharma, B.; Vaish, B.; Singh, U.K.; Singh, P.; Singh, R.P. Recycling of Organic Wastes in Agriculture: An Environmental Perspective. *Int. J. Env. Res.* **2019**, *13*, 409–429. [CrossRef]
6. Casabar, J.T.; Ramaraj, R.; Tipnee, S.; Unpaprom, Y. Enhancement of Hydrolysis with *Trichoderma Harzianum* for Bioethanol Production of Sonicated Pineapple Fruit Peel. *Fuel* **2020**, *279*, 118437. [CrossRef]
7. Basumatary, B.; Basumatary, S.; Das, B.; Nath, B.; Kalita, P. Waste *Musa Paradisiaca* Plant: An Efficient Heterogeneous Base Catalyst for Fast Production of Biodiesel. *J. Clean. Prod.* **2021**, *305*, 127089. [CrossRef]
8. Freitas, P.A.V.; González-Martínez, C.; Chiralt, A. Application of Ultrasound Pre-Treatment for Enhancing Extraction of Bioactive Compounds from Rice Straw. *Foods* **2020**, *9*, 1657. [CrossRef]
9. Prakash, A.; Vadivel, V.; Banu, S.F.; Nithyanand, P.; Lalitha, C.; Brindha, P. Evaluation of Antioxidant and Antimicrobial Properties of Solvent Extracts of Agro-Food by-Products (Cashew Nut Shell, Coconut Shell and Groundnut Hull). *Agric. Nat. Resour.* **2018**, *52*, 451–459. [CrossRef]
10. Ilyas, R.A.; Sapuan, S.M.; Ibrahim, R.; Abral, H.; Ishak, M.R.; Zainudin, E.S.; Atikah, M.S.N.; Mohd Nurazzi, N.; Atiqah, A.; Ansari, M.N.M.; et al. Effect of Sugar Palm Nanofibrillated Cellulose Concentrations on Morphological, Mechanical and Physical Properties of Biodegradable Films Based on Agro-Waste Sugar Palm (*Arenga Pinnata* (Wurmb.) Merr) Starch. *J. Mater. Res. Technol.* **2019**, *8*, 4819–4830. [CrossRef]
11. Kassab, Z. Cellulosic Materials from Pea (*Pisum Sativum*) and Broad Beans (*Vicia Faba*) Pods Agro-Industrial Residues. *Mater. Lett.* **2020**, *280*, 128–539. [CrossRef]
12. De Souza Lima, M.M.; Borsali, R. Rodlike Cellulose Microcrystals: Structure, Properties, and Applications. *Macromol. Rapid Commun.* **2004**, *25*, 771–787. [CrossRef]
13. FAOSTAT. Available online: <http://www.fao.org/faostat/en/#data/QC/visualize> (accessed on 4 November 2020).
14. Peanparkdee, M.; Iwamoto, S. Bioactive Compounds from By-Products of Rice Cultivation and Rice Processing: Extraction and Application in the Food and Pharmaceutical Industries. *Trends Food Sci. Technol.* **2019**, *86*, 109–117. [CrossRef]
15. Sarkar, N.; Ghosh, S.K.; Bannerjee, S.; Aikat, K. Bioethanol Production from Agricultural Wastes: An Overview. *Renew. Energy* **2012**, *37*, 19–27. [CrossRef]

16. El-Tayeb, T.S.; Abdelhafez, A.A.; Ali, S.H.; Ramadan, E.M. Effect of Acid Hydrolysis and Fungal Biotreatment on Agro-Industrial Wastes for Obtainment of Free Sugars for Bioethanol Production. *Braz. J. Microbiol.* **2012**, *43*, 1523–1535. [[CrossRef](#)] [[PubMed](#)]
17. Neto, W.P.F.; Silvério, H.A.; Vieira, J.G.; da Costa e Silva Alves, H.; Pasquini, D.; de Assunção, R.M.N.; Dantas, N.O. Preparation and Characterization of Nanocomposites of Carboxymethyl Cellulose Reinforced with Cellulose Nanocrystals. *Macromol. Symp.* **2012**, *319*, 93–98. [[CrossRef](#)]
18. Galdeano, M.C.; Mali, S.; Grossmann, M.V.E.; Yamashita, F.; García, M.A. Effects of Plasticizers on the Properties of Oat Starch Films. *Mater. Sci. Eng. C* **2009**, *29*, 532–538. [[CrossRef](#)]
19. Forssell, P.; Lahtinen, R.; Lahelin, M.; Myllä-Erinen, P. Oxygen Permeability of Amylose and Amylopectin Films. *Carbohydr. Polym.* **2002**, *47*, 125–129. [[CrossRef](#)]
20. Zainuddin, S.Y.Z. Potential of Using Multiscale Kenaf Fibers as Reinforcing Filler in Cassava Starch-Kenaf Biocomposites. *Carbohydr. Polym.* **2013**, *92*, 2299–2305. [[CrossRef](#)]
21. Carvalho, A.J.F. Starch: Major Sources, Properties and Applications as Thermoplastic Materials. In *Monomers, Polymers and Composites from Renewable Resources*; Elsevier: Amsterdam, The Netherlands, 2008; pp. 321–342, ISBN 978-0-08-045316-3.
22. González, K.; Retegi, A.; González, A.; Eceiza, A.; Gabilondo, N. Starch and Cellulose Nanocrystals Together into Thermoplastic Starch Bionanocomposites. *Carbohydr. Polym.* **2015**, *117*, 83–90. [[CrossRef](#)]
23. Teixeira, E.d.M.; Pasquini, D.; Curvelo, A.A.S.; Corradini, E.; Belgacem, M.N.; Dufresne, A. Cassava Bagasse Cellulose Nanofibrils Reinforced Thermoplastic Cassava Starch. *Carbohydr. Polym.* **2009**, *78*, 422–431. [[CrossRef](#)]
24. Collazo-Bigliardi, S. Isolation and Characterisation of Microcrystalline Cellulose and Cellulose Nanocrystals from Coffee Husk and Comparative Study with Rice Husk. *Carbohydr. Polym.* **2018**, *191*, 205–215. [[CrossRef](#)]
25. Ghanbarzadeh, B.; Almasi, H.; Entezami, A.A. Improving the Barrier and Mechanical Properties of Corn Starch-Based Edible Films: Effect of Citric Acid and Carboxymethyl Cellulose. *Ind. Crop. Prod.* **2011**, *33*, 229–235. [[CrossRef](#)]
26. Othman, S.H.; Majid, N.A.; Tawakkal, I.S.M.A.; Basha, R.K.; Nordin, N.; Shapi'i, R.A. Tapioca Starch Films Reinforced with Microcrystalline Cellulose for Potential Food Packaging Application. *Food Sci. Technol.* **2019**, *39*, 605–612. [[CrossRef](#)]
27. Chen, J.; Wang, X.; Long, Z.; Wang, S.; Zhang, J.; Wang, L. Preparation and Performance of Thermoplastic Starch and Microcrystalline Cellulose for Packaging Composites: Extrusion and Hot Pressing. *Int. J. Biol. Macromol.* **2020**, *165*, 2295–2302. [[CrossRef](#)] [[PubMed](#)]
28. Kargarzadeh, H. Starch Biocomposite Film Reinforced by Multiscale Rice Husk Fiber. *Compos. Sci. Technol.* **2017**, *151*, 147–155. [[CrossRef](#)]
29. Syafri, E.; Wahono, S.; Irwan, A.; Asrofi, M.; Sari, N.H.; Fudholi, A. Characterization and Properties of Cellulose Microfibers from Water Hyacinth Filled Sago Starch Biocomposites. *Int. J. Biol. Macromol.* **2019**, *137*, 119–125. [[CrossRef](#)] [[PubMed](#)]
30. Abdul Khalil, H.P.S.; Bhat, A.H.; Ireana Yusra, A.F. Green Composites from Sustainable Cellulose Nanofibrils: A Review. *Carbohydr. Polym.* **2012**, *87*, 963–979. [[CrossRef](#)]
31. Chandanasree, D.; Gul, K.; Riar, C.S. Effect of Hydrocolloids and Dry Heat Modification on Physicochemical, Thermal, Pasting and Morphological Characteristics of Cassava (*Manihot Esculenta*) Starch. *Food Hydrocoll.* **2016**, *52*, 175–182. [[CrossRef](#)]
32. Oh, I.K.; Bae, I.Y.; Lee, H.G. Effect of Dry Heat Treatment on Physical Property and in Vitro Starch Digestibility of High Amylose Rice Starch. *Int. J. Biol. Macromol.* **2018**, *108*, 568–575. [[CrossRef](#)]
33. Maniglia, B.C.; Lima, D.C.; Matta Junior, M.D.; Le-Bail, P.; Le-Bail, A.; Augusto, P.E.D. Preparation of Cassava Starch Hydrogels for Application in 3D Printing Using Dry Heating Treatment (DHT): A Prospective Study on the Effects of DHT and Gelatinization Conditions. *Food Res. Int.* **2020**, *128*, 108803. [[CrossRef](#)] [[PubMed](#)]
34. Sun, Q.; Xu, Y.; Xiong, L. Effect of Microwave-Assisted Dry Heating with Xanthan on Normal and Waxy Corn Starches. *Int. J. Biol. Macromol.* **2014**, *68*, 86–91. [[CrossRef](#)] [[PubMed](#)]
35. Freitas, P.A.V.; González-Martínez, C.; Chiralt, A. Applying ultrasound-assisted processing to obtain cellulose fibers from rice straw to be used as reinforcing agents. *Innov. Food Sci. Emerg. Technol.* **2021**, in press.
36. Collazo-Bigliardi, S.; Ortega-Toro, R.; Chiralt Boix, A. Reinforcement of Thermoplastic Starch Films with Cellulose Fibres Obtained from Rice and Coffee Husks. *J. Renew. Mater.* **2018**, *6*, 599–610. [[CrossRef](#)]
37. Rojas-Lema, S.; Quiles-Carrillo, L.; Garcia-Garcia, D.; Melendez-Rodriguez, B.; Balart, R.; Torres-Giner, S. Tailoring the Properties of Thermo-Compressed Polylactide Films for Food Packaging Applications by Individual and Combined Additions of Lactic Acid Oligomer and Halloysite Nanotubes. *Molecules* **2020**, *25*, 1976. [[CrossRef](#)]
38. Talón, E.; Trifkovic, K.T.; Nedovic, V.A.; Bugarski, B.M.; Vargas, M.; Chiralt, A.; González-Martínez, C. Antioxidant Edible Films Based on Chitosan and Starch Containing Polyphenols from Thyme Extracts. *Carbohydr. Polym.* **2017**, *157*, 1153–1161. [[CrossRef](#)]
39. McHugh, T.H.; Avena-Bustillos, R.; Krochta, J.M. Hydrophilic Edible Films: Modified Procedure for Water Vapor Permeability and Explanation of Thickness Effects. *J. Food Sci.* **1993**, *58*, 899–903. [[CrossRef](#)]
40. Collazo-Bigliardi, S.; Ortega-Toro, R.; Chiralt, A. Improving Properties of Thermoplastic Starch Films by Incorporating Active Extracts and Cellulose Fibres Isolated from Rice or Coffee Husk. *Food Packag. Shelf Life* **2019**, *22*, 100383. [[CrossRef](#)]
41. Jin, S.; Chen, H. Structural Properties and Enzymatic Hydrolysis of Rice Straw. *Process Biochem.* **2006**, *41*, 1261–1264. [[CrossRef](#)]
42. Zhang, Z.; Smith, C.; Li, W. Extraction and Modification Technology of Arabinoxylans from Cereal By-Products: A Critical Review. *Food Res. Int.* **2014**, *65*, 423–436. [[CrossRef](#)]
43. Cheung, Y.-C.; Wu, J.-Y. Kinetic Models and Process Parameters for Ultrasound-Assisted Extraction of Water-Soluble Components and Polysaccharides from a Medicinal Fungus. *Biochem. Eng. J.* **2013**, *79*, 214–220. [[CrossRef](#)]

44. Hayat, K.; Abbas, S.; Hussain, S.; Shahzad, S.A.; Tahir, M.U. Effect of Microwave and Conventional Oven Heating on Phenolic Constituents, Fatty Acids, Minerals and Antioxidant Potential of Fennel Seed. *Ind. Crop. Prod.* **2019**, *140*, 111610. [[CrossRef](#)]
45. Machado, I. Characterization of the Effects Involved in Ultrasound-Assisted Extraction of Trace Elements from Artichoke Leaves and Soybean Seeds. *Ultrason. Sonochem.* **2019**, *59*, 104752. [[CrossRef](#)]
46. Moslemi, A. Addition of Cellulose Nanofibers Extracted from Rice Straw to Urea Formaldehyde Resin; Effect on the Adhesive Characteristics and Medium Density Fiberboard Properties. *Int. J. Adhes. Adhes.* **2020**, *99*, 102582. [[CrossRef](#)]
47. Bocek, A.M. Effect of Hydrogen Bonding on Cellulose Solubility in Aqueous and Nonaqueous Solvents. *Russ. J. Appl. Chem.* **2003**, *76*, 1711–1719. [[CrossRef](#)]
48. Jiang, F.; Han, S.; Hsieh, Y.-L. Controlled Defibrillation of Rice Straw Cellulose and Self-Assembly of Cellulose Nanofibrils into Highly Crystalline Fibrous Materials. *RSC Adv.* **2013**, *3*, 12366. [[CrossRef](#)]
49. Littunen, K.; Hippi, U.; Saarinen, T.; Seppälä, J. Network Formation of Nanofibrillated Cellulose in Solution Blended Poly(Methyl Methacrylate) Composites. *Carbohydr. Polym.* **2013**, *91*, 183–190. [[CrossRef](#)]
50. Hernández-García, E.; Vargas, M.; Chiralt, A. Thermoprocessed Starch-Polyester Bilayer Films as Affected by the Addition of Gellan or Xanthan Gum. *Food Hydrocoll.* **2021**, *113*, 106509. [[CrossRef](#)]
51. Menzel, C.; González-Martínez, C.; Vilaplana, F.; Diretto, G.; Chiralt, A. Incorporation of Natural Antioxidants from Rice Straw into Renewable Starch Films. *Int. J. Biol. Macromol.* **2020**, *146*, 976–986. [[CrossRef](#)] [[PubMed](#)]
52. Oladebeye, A.O.; Oshodi, A.A.; Amoo, I.A.; Karim, A.A. Functional, Thermal and Molecular Behaviours of Ozone-Oxidised Cocoyam and Yam Starches. *Food Chem.* **2013**, *141*, 1416–1423. [[CrossRef](#)] [[PubMed](#)]
53. Abraham, E. Extraction of Nanocellulose Fibrils from Lignocellulosic Fibres: A Novel Approach. *Carbohydr. Polym.* **2011**, *86*, 1468–1475. [[CrossRef](#)]
54. Hung, P.V.; My, N.T.H.; Phi, N.T.L. Impact of Acid and Heat-Moisture Treatment Combination on Physicochemical Characteristics and Resistant Starch Contents of Sweet Potato and Yam Starches. *Starch—Stärke* **2014**, *66*, 1013–1021. [[CrossRef](#)]
55. Benito-González, I.; López-Rubio, A.; Martínez-Sanz, M. High-Performance Starch Biocomposites with Cellulose from Waste Biomass: Film Properties and Retrogradation Behaviour. *Carbohydr. Polym.* **2019**, *216*, 180–188. [[CrossRef](#)]
56. Fourati, Y.; Magnin, A.; Putaux, J.-L.; Boufi, S. One-Step Processing of Plasticized Starch/Cellulose Nanofibrils Nanocomposites via Twin-Screw Extrusion of Starch and Cellulose Fibers. *Carbohydr. Polym.* **2020**, *229*, 115554. [[CrossRef](#)]
57. Lim, H.S.; Han, J.-A.; BeMiller, J.N.; Lim, S.-T. Physical Modification of Waxy Maize Starch by Dry Heating with Ionic Gums. *J. Appl. Glycosci.* **2006**, *53*, 281–286. [[CrossRef](#)]
58. Ma, X.; Yu, J.; Kennedy, J.F. Studies on the Properties of Natural Fibers-Reinforced Thermoplastic Starch Composites. *Carbohydr. Polym.* **2005**, *62*, 19–24. [[CrossRef](#)]
59. Avérous, L.; Fringant, C.; Moro, L. Plasticized Starch–Cellulose Interactions in Polysaccharide Composites. *Polymer* **2001**, *42*, 6565–6572. [[CrossRef](#)]
60. El Halal, S.L.M.; Colussi, R.; Deon, V.G.; Pinto, V.Z.; Villanova, F.A.; Carreño, N.L.V.; Dias, A.R.G.; Zavareze, E.d.R. Films Based on Oxidized Starch and Cellulose from Barley. *Carbohydr. Polym.* **2015**, *133*, 644–653. [[CrossRef](#)] [[PubMed](#)]
61. Müller, C.M.O.; Laurindo, J.B.; Yamashita, F. Effect of Cellulose Fibers Addition on the Mechanical Properties and Water Vapor Barrier of Starch-Based Films. *Food Hydrocoll.* **2009**, *23*, 1328–1333. [[CrossRef](#)]
62. Cornejo-Ramírez, Y.I.; Martínez-Cruz, O.; Del Toro-Sánchez, C.L.; Wong-Corral, F.J.; Borboa-Flores, J.; Cinco-Moroyoqui, F.J. The Structural Characteristics of Starches and Their Functional Properties. *Cyta—J. Food* **2018**, *16*, 1003–1017. [[CrossRef](#)]
63. Talja, R.A.; Helén, H.; Roos, Y.H.; Jouppila, K. Effect of Various Polyols and Polyol Contents on Physical and Mechanical Properties of Potato Starch-Based Films. *Carbohydr. Polym.* **2007**, *67*, 288–295. [[CrossRef](#)]
64. Hedenqvist, M.S. Barrier Packaging Materials. In *Handbook of Environmental Degradation of Materials*; Elsevier: Amsterdam, The Netherlands, 2012; pp. 833–862, ISBN 978-1-4377-3455-3.
65. Fazeli, M.; Keley, M.; Biazar, E. Preparation and Characterization of Starch-Based Composite Films Reinforced by Cellulose Nanofibers. *Int. J. Biol. Macromol.* **2018**, *116*, 272–280. [[CrossRef](#)]
66. Li, Y.; Shoemaker, C.F.; Ma, J.; Shen, X.; Zhong, F. Paste Viscosity of Rice Starches of Different Amylose Content and Carboxymethyl-cellulose Formed by Dry Heating and the Physical Properties of Their Films. *Food Chem.* **2008**, *109*, 616–623. [[CrossRef](#)]
67. Reyes, I.; Hernandez-Jaimes, C.; Vernon-Carter, E.J.; Bello-Perez, L.A.; Alvarez-Ramirez, J. Air Oxidation of Corn Starch: Effect of Heating Temperature on Physicochemical Properties and In Vitro Digestibility. *Starch—Stärke* **2021**, *73*, 2000237. [[CrossRef](#)]
68. Zamudio-Flores, P.B.; Vargas-Torres, A.; Pérez-González, J.; Bosquez-Molina, E.; Bello-Pérez, L.A. Films Prepared with Oxidized Banana Starch: Mechanical and Barrier Properties. *Starch—Stärke* **2006**, *58*, 274–282. [[CrossRef](#)]
69. Adeyi, A.J.; Durowoju, M.O.; Adeyi, O.; Oke, E.O.; Olalere, O.A.; Ogunsola, A.D. Momordica Augustisepala L. Stem Fibre Reinforced Thermoplastic Starch: Mechanical Property Characterization and Fuzzy Logic Artificial Intelligent Modelling. *Results Eng.* **2021**, *10*, 100222. [[CrossRef](#)]
70. Lu, Y.; Weng, L.; Cao, X. Biocomposites of Plasticized Starch Reinforced with Cellulose Crystallites from Cottonseed Linter. *Macromol. Biosci.* **2005**, *5*, 1101–1107. [[CrossRef](#)]
71. Maria, V.D.; Bernal, C.; Francois, N.J. Development of Biodegradable Films Based on Chitosan/Glycerol Blends Suitable for Biomedical Applications. *J. Tissue Sci. Eng.* **2016**, *7*. [[CrossRef](#)]
72. Merci, A.; Marim, R.G.; Urbano, A.; Mali, S. Films Based on Cassava Starch Reinforced with Soybean Hulls or Microcrystalline Cellulose from Soybean Hulls. *Food Packag. Shelf Life* **2019**, *20*, 100321. [[CrossRef](#)]

-
73. Melendez-Rodriguez, B.; Torres-Giner, S.; Aldureid, A.; Cabedo, L.; Lagaron, J.M. Reactive Melt Mixing of Poly(3-Hydroxybutyrate)/Rice Husk Flour Composites with Purified Biosustainably Produced Poly(3-Hydroxybutyrate-Co-3-Hydroxyvalerate). *Materials* **2019**, *12*, 2152. [[CrossRef](#)]
 74. Menzel, C.; González-Martínez, C.; Chiralt, A.; Vilaplana, F. Antioxidant Starch Films Containing Sunflower Hull Extracts. *Carbohydr. Polym.* **2019**, *214*, 142–151. [[CrossRef](#)] [[PubMed](#)]